Protein phosphatase 4 is phosphorylated and inactivated by Cdk in response to spindle toxins and interacts with γ-tubulin

Martin Voss[†], Kathryn Campbell[†], Nastja Saranzewa[†], David G Campbell, C James Hastie, Mark W Peggie, Cristina Martin-Granados, Alan R Prescott, and Patricia TW Cohen*

Medical Research Council Protein Phosphorylation and Ubiquitylation Unit; College of Life Sciences; University of Dundee; Dundee, Scotland, UK

[†]These authors have contributed the major experimental data in the article.

Many pharmaceuticals used to treat cancer target the cell cycle or mitotic spindle dynamics, such as the anti-tumor drug, paclitaxel, which stabilizes microtubules. Here we show that, in cells arrested in mitosis with the spindle toxins, nocodazole, or paclitaxel, the endogenous protein phosphatase 4 (Ppp4) complex Ppp4c-R2-R3A is phosphorylated on its regulatory (R) subunits, and its activity is inhibited. The phosphorylations are blocked by roscovitine, indicating that they may be mediated by Cdk1-cyclin B. Endogenous Ppp4c is enriched at the centrosomes in the absence and presence of paclitaxel, nocodazole, or roscovitine, and the activity of endogenous Ppp4c-R2-R3A is inhibited from G_1/S to the G_2/M phase of the cell cycle. Endogenous γ-tubulin and its associated protein, γ-tubulin complex protein 2, both of which are essential for nucleation of microtubules at centrosomes, interact with the Ppp4 complex. Recombinant γ-tubulin can be phosphorylated by Cdk1-cyclin B or Brsk1 and dephosphorylated by Ppp4c-R2-R3A in vitro. The data indicate that Ppp4c-R2-R3A regulates microtubule organization at centrosomes during cell division in response to stress signals such as spindle toxins, paclitaxel, and nocodazole, and that inhibition of the Ppp4 complex may be advantageous for treatment of some cancers.

Introduction

Co-ordination of the processes that regulate cell division is essential for cell proliferation and survival, and an understanding of these mechanisms may lead to the identification of novel anticancer targets. Major chemotherapeutic agents such as paclitaxel, used for the treatment of solid tumors, including breast, ovarian, gastroesophageal, head and neck cancers, target the mitotic spindle.[1] One process of great interest, which is essential for the formation of the mitotic spindle, is the nucleation of microtubules at the centrosomes. Although microtubules are composed of α- and β-tubulin heterodimers, γ-tubulin, a homolog enriched in the pericentriolar material surrounding the centrosome, is essential for the initiation of microtubule growth in all organisms studied.[2-4] In mammals, centrosomal γ-tubulin is associated with at least 9 proteins that form a ring-shaped structure, termed γ-tubulin ring complex (γTuRC), which can be dissociated to release a smaller complex (γTuSC) comprising 2 molecules of γ-tubulin, one molecule of γ-tubulin complex protein (TUBGCP)2 and one TUBGCP3.[5] Although γTuSC is sufficient for microtubule nucleation in vitro and in yeast, the assembly of several γTuSC into the larger γTuRC structure achieves increased microtubule nucleation in metazoans by the addition of GCP4, GCP5, GCP6, and a few smaller proteins.[4,6] A spiral of 13 γ-tubulin molecules in seven γTuSC serves as a template to promote the polymerization of α-tubulin/β-tubulin heterodimers into 13 protofilaments, which form each microtubule in vitro and in vivo.[7,8] However, the biochemical mechanism(s) by which γ-tubulin nucleates microtubule growth is unknown.

Protein phosphatase 4 (Ppp4/PP4) is a ubiquitous protein phosphatase, and the catalytic subunit (Ppp4c) has been highly conserved during evolution. Located in both the cytoplasm and the nucleus, Ppp4c is noticeably enriched in the pericentriolar material in the mammalian cell during mitosis.[9] Embryos from a *Drosophila melanogaster* mutant (centrosomes minus microtubules, *cmm*) with low levels of Ppp4c showed nuclei blocked in mitosis with loss of microtubule attachment to the pericentriolar region and a decrease in γ-tubulin at the centrosome, suggesting that Ppp4 may regulate the nucleation of microtubule growth at centrosomes.[10] A similar phenotype was observed in *C. elegans* Ppp4c mutants,

where disorganization of Polo-like kinase (Plk) was also noted further supporting a role for Ppp4 in the nucleation of microtubules at centrosomes during mitosis.[11] Studies in the mouse demonstrate that Ppp4c is essential in higher eukaryotes,[12] and depletion of Ppp4c by lentiviral-mediated stable gene silencing in human embryonic kidney (HEK)293 cells caused a block at M phase of the cell cycle, with some cells displaying aberrant chromosomal organization and loss of microtubules near the centrosomes.[13]

A major form of Ppp4 found in organisms from yeast to man comprises Ppp4c in complex with a core regulatory subunit R2, and a variable regulatory subunit R3.[14-16] Although *S. cerevisiae* has only one form of R3, in human cells there are 2 isozymes, R3A and R3B. Immunocytological analyses have shown that R2 and R3A are enriched in the pericentriolar material during mitosis in human cells.[13,17,18] In this article, we analyze the phosphorylation and associated activity of endogeneous Ppp4c–R2–R3A complex during the cell cycle in untreated human cells and in cell cultures arrested at G_2/M by nocodazole or paclitaxel. We also identify and investigate interaction of the endogenous Ppp4 complex with γ-tubulin and its associated proteins in γTuSC.

Results

Analysis of regulatory phosphorylation sites in the R2 regulatory subunit of Ppp4

The regulation of Ppp4-R2-R3A complex was examined by expression of FLAG-tagged R2 in HEK293 cells treated with nocodazole, which causes cell cycle arrest at G_2/M. Analysis of FLAG-R2 peptides by tandem mass spectrometry revealed several phosphopeptides, and the relative amount of each phosphorylated peptide was assessed by comparison with other R2 peptides. Two peptides, one encompassing R2pSer159 (m/z 948.5) containing 2 methionine sulphoxide residues and the other R2pThr173 (m/z 898.5), were not evident in untreated HEK293 cells, but were very clearly detected after nocodazole treatment (**Fig. 1A**). The ions (m/z 933.5 and 941.5) are the non-oxidized and singly oxidized versions of the R2pSer159 peptide (m/z 948.5). In contrast, the non-phosphorylated N-terminal FLAG-tag peptide and another R2 peptide, encompassing pSer226, at 1027.6, were clearly present in untreated cells and did not increase in amount after nocodazole treatment. The results suggested that R2pSer159 and R2pThr173 may control the response to nocodazole, while R2pSer226 is unlikely to be involved. Antibodies were raised to R2pSer159 and R2pThr173, and also R3ApSer741, which was found to be phosphorylated in asynchronous HEK293 cells transfected with FLAG-R3A.

Although other serine or threonine residues in R2 (one Ser/Thr in amino acids 269–289; Ser388 or 389) and R3A (one or more serines among the amino acids 768–783) were phosphorylated in nocodazole-treated cells, it was not possible to raise specific antibodies to these sites, and they were not further investigated.

Effect of spindle toxins and kinase inhibitors on the phosphorylation and subcellular localization of endogenous Ppp4c, R2, and R3A

Treatment of HEK293 and HeLa cells with nocodazole, a microtubule-depolymerizing agent, and paclitaxel, a microtubule-stabilizing drug,[19,20] blocked the cell cycle at G_2/M and resulted in increased phosphorylation of endogenous R2Ser159, R2Thr173, and R3ASer741 (**Fig. 1B and C**). In contrast, roscovitine, a Cdk inhibitor that also blocks the cell cycle at G_2/M caused no increase in phosphorylation of these sites compared with that in untreated cells. Furthermore, the differences are evident, not only with antibodies against the phosphosites, but also with R2 and R3A antibodies, which reveal that endogenous R3A and R2 migrate more slowly when phosphorylated at G_2/M in response to nocodazole and paclitaxel. The migration and expression of the catalytic subunit Ppp4c, was not altered by the cell cycle blocks (**Fig. 1B and C**).

Although the phosphospecific antibodies were not sensitive enough to be employed for immunocytochemistry, antibodies to Ppp4c and R3A detected the subcellular localizations of these proteins in cells treated with cell cycle inhibitors. Ppp4c and R3A were enriched in HeLa cells in the pericentriolar region during mitosis, and prior incubation of the antibodies with the peptide antigen resulted in loss of this localization, demonstrating antibody specificity (**Fig. 2**). Treatment of cells with nocodazole, paclitaxel, or roscovitine did not affect the enrichment of Ppp4c in the pericentriolar region in metaphase (**Fig. 2**) and anaphase (not shown). At telophase, Ppp4c was absent or only weakly present in the centrosomal region in control and treated cells. Since pericentrosomal enrichments of Ppp4c were observed in cells treated with spindle toxins that increase, and roscovtine that blocks, R2 and R3A phosphorylations, these modifications do not therefore control the subcellular localization of Ppp4c.

Pericentriolar localization of R3A was only observed in 65% of control cells in mitosis as observed previously,[13] and this was decreased to 35% on treatment with roscovitine (**Fig. 2**), suggesting differential subcellular distribution of R3A with respect to Ppp4c may occur. However, anti-R3A and anti-R2 antibodies have much lower affinity than the anti-Ppp4c antibodies, and therefore low levels are difficult to detect.

Treatment of HEK293 cells with a variety of kinase inhibitors for 1 h prior to the end of 16 h nocodazole treatment (**Fig. 3**) or 1 h prior to the start and during 16 h nocodazole treatment (data not shown) had no effect on the phosphorylation of R2Ser159, R2Thr173, or R3ASer741. These included 2.0 μM PD 0325901, which inhibits ERK1, ERK2, and ERK5, 10 μM BIRB 0796, which inhibits p38 MAPK and JNK1, 2, and 3, 1.0 μM PI-103, which inhibits PI 3-kinase and mTOR, 2 μM GDC 0941, which inhibits PI 3-kinase more specifically than PI-103, because it does not inhibit mTOR, or 10 μM harmine, which inhibits DYRK. However, 25 μM roscovitine blocked the phosphorylations (**Figs. 1B and C and 3C and D**). The data eliminate many signaling pathways in mediating the phosphorylation of R2Ser159, R2Thr173, and R3ASer741 and indicate that the phosphorylations are performed by a Cdk at the G_2–M transition, implicating Cdk1-cyclin B, which is maximally induced at this stage of the cell cycle.

Phosphorylation of endogenous R2 and R3A during the cell cycle

To determine whether the regulatory subunits of endogenous Ppp4c-R2-R3A were phosphorylated during the cell cycle, HeLa

and HEK293 cells were synchronized at G_1/S by a double thymidine block and allowed to continue the cell cycle in the absence of G_2/M inhibitors. Analysis of HeLa cells by flow cytometry[13] showed the cells passed synchronously from G_2 to M phase 10 h after release from the second thymidine block. Immunoblotting of the HeLa cell lysates showed that histone H3Ser10 was phosphorylated, as expected at G_2/M (**Fig. 4A and D**). R2 migrated as 2 bands in asynchronous HeLa cell lysates analyzed on 6% polyacrylamide gels, but mainly as the more slowly migrating

band between the double thymidine block to 10 h after release, suggesting R2 was phosphorylated during this period (**Fig. 4D**). Twelve–14 h after release from the double thymidine block, the faster migrating band gradually reappeared as cells passed into G_1 marked by increase of cyclin E1 (**Fig. 4D**). Although increased phosphorylation of endogenous R2 at specific sites was technically difficult to detect during the cell cycle, probably because of transitory low levels, phosphorylation of R2Thr173 was observed 10 h after release from the double thymidine block
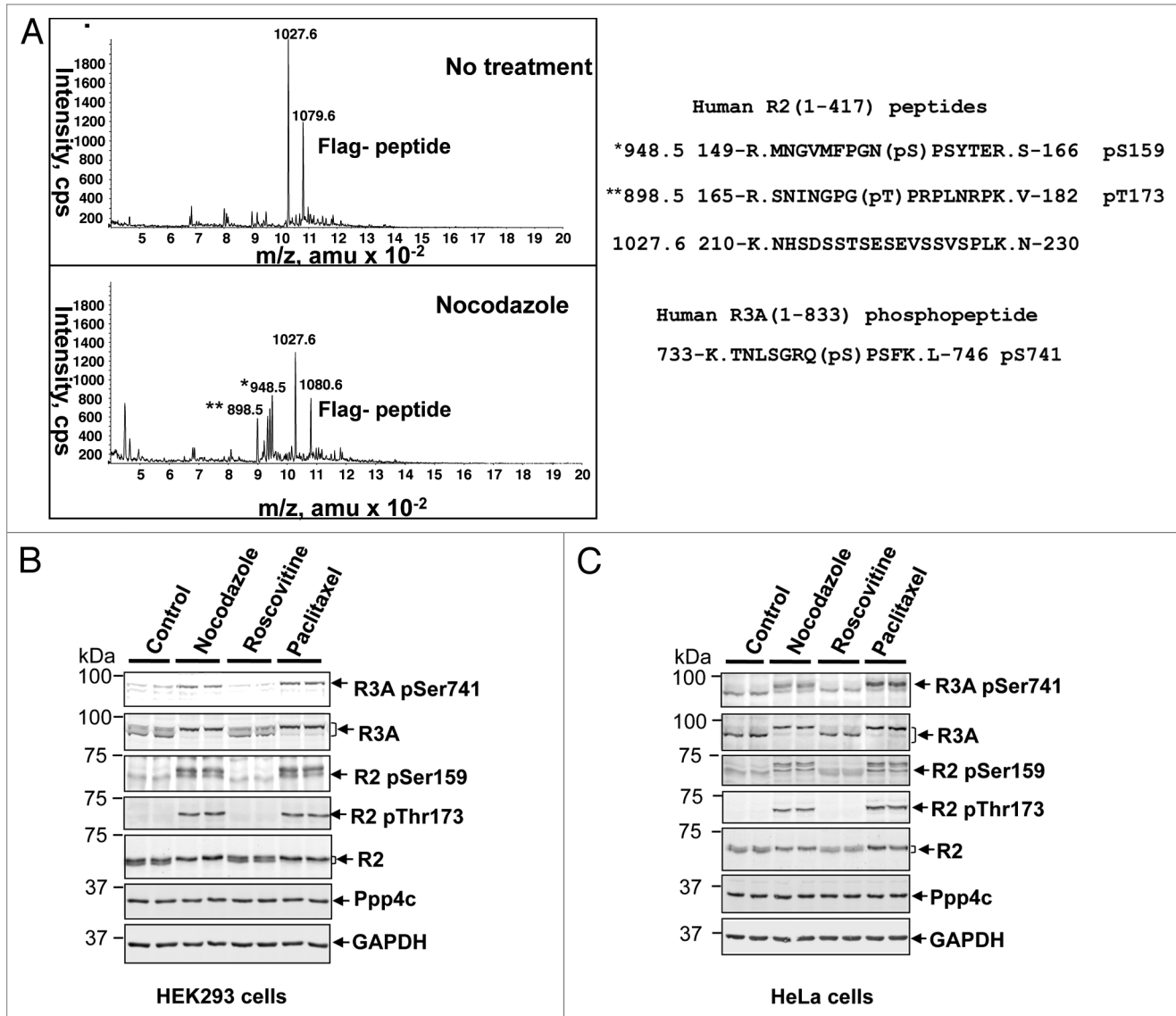

Figure 1. Phosphorylation of the regulatory subunits of Ppp4c in response to spindle toxins and a cell cycle inhibitor. (**A**) Human FLAG-R2 was expressed in HEK293 cells cultured with or without nocodazole treatment for 16 h. Cells were lysed in lysis buffer containing phosphatase inhibitor. FLAG-tagged R2 was immunoadsorbed from the cell lysates and the proteins in the immunopellets separated by gel electrophoresis. The R2 protein band was cut out of the gel, digested with trypsin, and the R2 peptides were analyzed for phosphorylation by precursor ion scanning. The spectra show 2 phosphorylated R2 peptides that are present in nocodazole-treated samples and virtually absent in untreated controls, while a third R2 peptide and the FLAG peptide are present at similar levels in untreated and nocodazole-treated samples. The ion at m/z 448.2 was singly charged and did not correspond to the mass of any expected peptide from R2. The sequences of the R2 peptides are presented on the right. The sequence of a R3A phosphorylated peptide, which was also identified after treatment of cells with nocodazole, is shown below. m/z, mass/charge; amu, atomic mass units; cps, counts per second. (**B and C**) Phosphorylation of endogenous R2 and R3A in response to cell cycle inhibitors in HEK293 and HeLa cells, untreated (control) or treated with 300 nM nocodazole, 25 μM roscovitine or 33 nM paclitaxel for 16 h. Proteins in the cell lysates were separated by SDS gel electrophoresis, transferred to nitrocellulose membranes and probed with antibodies to the indicated proteins. Size markers in kDa are shown on the left. The predicted molecular sizes are human R3A 95.4 kDa, R2 46.9 kDa and Ppp4c 35.1 kDa (Q6IN85, Q9N27, P60510 at http://www.uniprot.org/).

(**Fig. 4C and D**). Comparison of R2 immunopellets from lysates of HeLa and HEK293 asynchronous cultures with R2 immunopellets following release from a double thymidine block indicated that the phosphorylation of R2Ser159 may be slightly increased at the double thymidine block and clearly increased at the G_2/M (**Figs. 4B and 5B**). A small increase in R3ASer741 phosphorylation was observed in R2 immunopellets from HEK293 cell lysates 10 h after release from the double thymidine block (**Fig. 5A and B**).
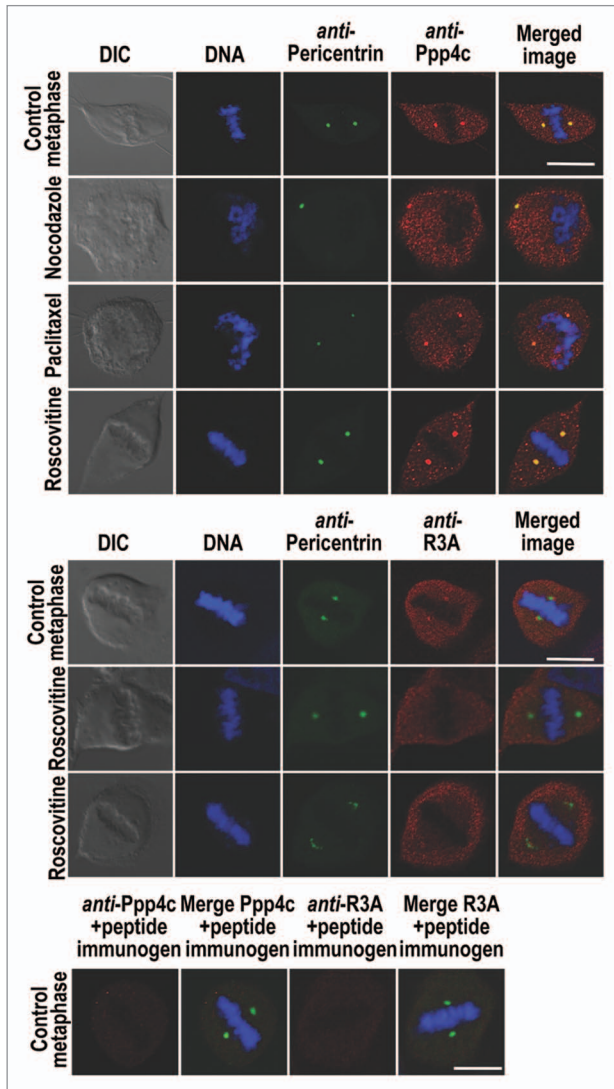

Figure 2. Effect of cell cycle inhibitors on the subcellular location of R2 and R3A. HeLa cells were fixed and initially viewed using differential interference contrast (DIC). DNA (blue) was stained with DAPI. Anti-pericentrin stain (green) identifies the pericentriolar material. Anti-Ppp4c(287–305) stain (red) in the top panel and anti-R3A(819–833) stain (red) in the middle panel identifies Ppp4c and R3A, respectively, as indicated. The top panel shows Ppp4c enrichment in the pericentriolar region in control and roscovitine-treated cells in metaphase and cells treated with nocodazole and paclitaxel. The middle panel shows R3A enrichment in the pericentriolar region (control) and the loss or partial loss of R3A from the pericentriolar region after treatment of the cells with roscovitine. Representative images are shown in each case. The bottom, panel shows the control images, where anti-Ppp4c or anti-R3A antibodies are blocked with their respective peptide immunogen. Scale bars are 10 μm.

These results imply that endogenous R3ASer741, R2Ser159, and R2Thr173 are transiently phosphorylated at G_2/M.

Activity of the Ppp4c–R2–R3A complex during the cell cycle

The activity of Ppp4 complexes was determined following adsorption with anti-R3A antibody from HEK293 cell lysates after release from a double thymidine block. (**Fig. 5C**). At S phase (0 h after release from the double thymidine block), Ppp4 activity decreased to half that observed in asynchronous cultures. Lower levels of activity are observed during G_2-phase (6 h after release) and M-phase (10 h after release). When the cells exit M-phase and return to G_1 (16 h after release) the Ppp4 activity increases more than 10-fold compared with that observed in G_2 and over 2-fold that determined in AS cultures. Treatment of cells with nocodazole or paclitaxel causes a profound decrease of Ppp4 activity to ~10% or less than that observed in G_1-phase. These results show that decrease in Ppp4 activity coincides with the phosphorylations of R2 and R3A.

In order to confirm the Ppp4 activity changes assayed in cell lysates, GST-R3A-His$_6$R2-Ppp4c was expressed in insect cells and purified using the GST tag. The main bands observed in the preparation after SDS gel electrophoresis were identified as GST-R3A, His$_6$R2, and Ppp4c by mass spectrometry and migrated at the sizes expected for these protein subunits (**Fig. 5D and E**). Following removal of phosphate with lambda protein phosphatase, assay of the recombinant GST-R3A-His$_6$R2-Ppp4c complex using RRApTVA as substrate gave an activity of 227 nmol phosphate released/mg protein/min. Phosphorylation of GST-R3A-His$_6$R2-Ppp4c with Cdk1-cyclin B decreased the activity to ~10% of that observed after λ phosphatase treatment. Immunoblotting identified R2Ser159, R2Thr173, and R3ASer741 as sites of phosphorylation by Cdk1-cyclin B (**Fig. 5D and E**).

Identification of proteins interacting with Ppp4c

Investigation of substrate(s) with which endogenous Ppp4c-R2-R3A may be interacting during the cell cycle was performed by immunoadsorption with anti-Ppp4c or anti-R3A antibodies in HEK293 cell lysates. Following electrophoretic separation, proteins in the immunopellets were analyzed by mass spectrometry. The top Ppp4c-interacting protein in ~50 kDa gel slice was γ-tubulin-1 (Mr 51 kDa, Uniprot P23258) from untreated asynchronous cultures and nocodazole- or paclitaxel-treated cells, and even in larger gel sections, γ-tubulin-1 was identified among the top 5 putative interactors. The γ-tubulin-1 sequence coverage was high in all analyses reaching 94%. γ-tubulin was also detected in anti-Ppp4c immunopellets by blotting and was barely detectable in controls in which the anti-Ppp4c antibody was blocked with peptide immunogen, demonstrating that the interaction was specific (**Fig. 6A**). In the ~100 kDa band of the anti-Ppp4c immunopellets, γ-tubulin complex component 2 (TubGCP2, 102.5 kDa, Uniprot Q9BSJ2) with a sequence coverage of 44% and γ-tubulin complex component 3 isoform 1 (TubGCP3, 103.6 kDa, Uniprot Q96CW5) with a sequence coverage of 32%, the two other proteins in the γ-tubulin small ring complex (γ-tubulin SC), were identified among the top 10 Ppp4c interacting proteins by mass spectrometry. Anti-R3A adsorption gave similar results, with γ-tubulin-1 being identified among

the top 5 putative interactors, and TubGCP2 and TubGCP3 being among the top 10 interacting proteins. In the anti-Ppp4c immunopellets, R3A was not detected and R2 was at lower levels than Ppp4c, suggesting that interaction with γ-tubulin was with Ppp4c or R2 rather than R3A.

Analysis of anti-Ppp4c pellets from HEK293 cells by immunoblotting confirmed the interaction with γ-tubulin and TUBGCP2 and showed that the γTuSC proteins were more loosely bound than R2 to Ppp4c. (**Fig. 6A and C**). No interaction with TUBGCP3 was detected. Investigation of the interaction of γ-tubulin with Ppp4c during the cell cycle following release from a double thymidine block showed a marked increase in γ-tubulin/α-tubulin ratio in the anti-Ppp4c immunopellets compared with the ratio in the HEK293 cell lysates (**Fig. 6B**). Disappointingly, analysis of the γ-tubulin in the anti-Ppp4c immunopellets by mass spectrometry did not reveal any phosphorylated sites, possibly because substrates bound to the phosphatase would be very rapidly dephosphorylated, and the phospho-forms would therefore be too small to be detected by mass spectrometry, or because the phospho-γ-tubulin does not bind to Ppp4c.

In order to identify putative phosphorylation sites on γ-tubulin, the His$_6$-tagged TUBG1 was phosphorylated with Cdk1-cyclin B or Brsk1 in vitro, and the His$_6$-γ-tubulin Ni^{2+}-pellets were then treated with Ppp4c-R2-R3A. Cdk1-cyclin B was chosen because of its inactivation of Ppp4c-R2-R3A demonstrated above, and Brsk1 because it is the only kinase reported to phosphorylate γ-tubulin (at Ser131).[21] The γ-tubulin phospho-sites in these samples were examined by SDS-PAGE followed by mass spectrometry. Cdk1-cyclin B phosphorylated Ser80 and Thr196, while Brsk1 phosphorylated Thr196 but not phospho-Ser131. Ppp4c-R2-R3A dephosphorylated γ-tubulin-pThr196 and 60% dephosphorylation of γ-tubulin-pSer80 was observed (**Fig. 6D and E**).

Discussion

Our data demonstrate for the first time how the activity of the phosphatase Ppp4c-R2-R3A is regulated during the cell cycle and identify interaction of this protein phosphatase complex with γ-tubulin and its associated protein TUBGCP2 in γ-TuSC, implicating Ppp4c-R2-R3A as a significant player coordinating the cell cycle and microtubule attachment to the centrosomes. Importantly, phosphorylation of the endogenous Ppp4c–R2–R3A complex is increased at G$_2$/M on R2Ser159, R2Thr173 and R3ASer741 in HEK293 and HeLa cells by treatment with the spindle toxins nocodazole and paclitaxel. Our studies also show transient increases in these phosphorylations in HeLa and HEK293 cells at G$_2$/M in the absence of any G$_2$/M inhibitor. Phosphorylation of R2Ser159

has been noted previously in nocodazole-treated HeLa cells[22] but not in the absence of a G$_2$/M inhibitor. R3ASer741 is partially phosphorylated in asynchronous cultures, consistent with a previous report.[23] Our demonstration that roscovitine, but not several other kinase inhibitors, can block the nocodazole-induced phosphorylation of these 3 amino acids on endogenous R2 and R3A in human cells, implicates a Cdk in mediating the phosphorylations. All the sites identified are Ser or Thr followed by Pro, consistent with them being Cdk phosphorylation sites. Although several Cdks (Cdk1, Cdk2, Cdk5, Cdk7, Cdk9) are inhibited by
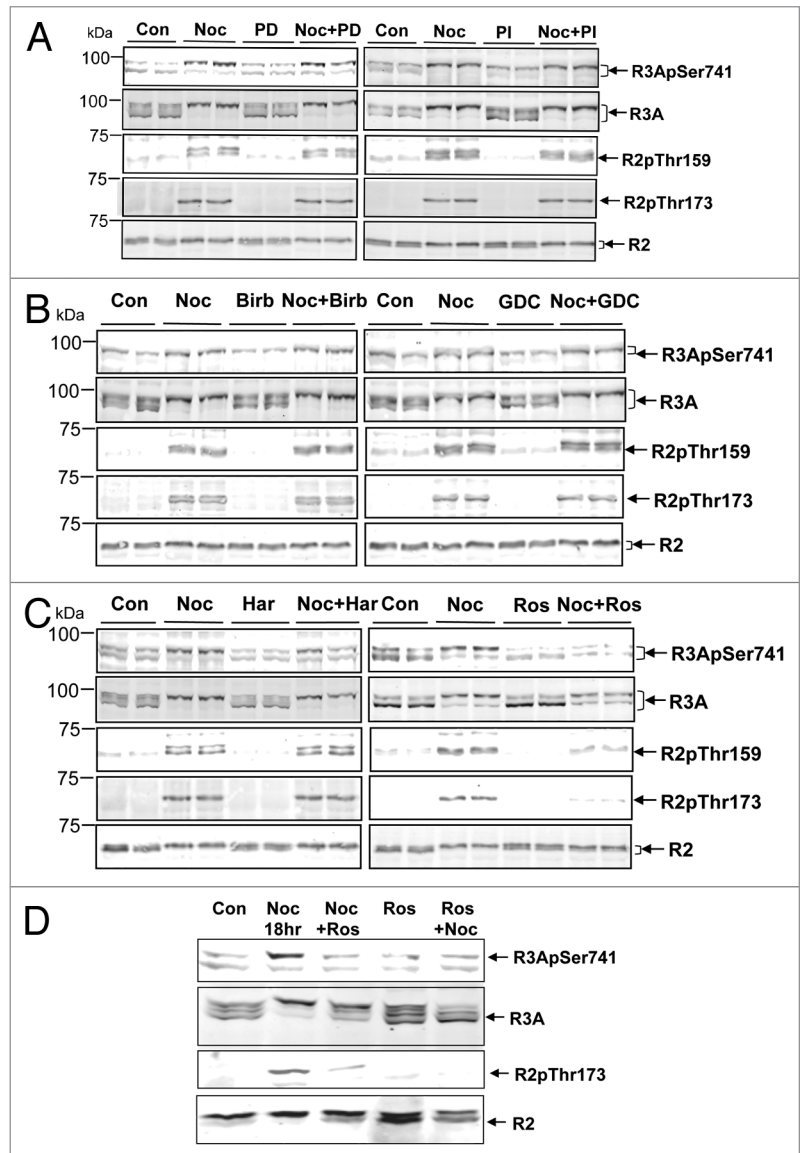

Figure 3. Effect of kinase inhibitors on the nocodazole-induced phosphorylation of endogenous R2 and R3A in HEK293 cells. (**A–D**) HEK293 cells at 60–80% confluence were cultured at 37 °C untreated (con) or treated with 300 nM nocodazole (Noc) for 16 h. The following protein kinase inhibitors were added to the culture medium to the stated concentrations 1 h prior to the end of the nocodazole treatment: 10 μM BIRB 0796 (BIRB); 2 μM PD 0325901 (PD); 1 μM PI-103; 2 μM GDC-0941 (GDC); 10 μM Harmine (Har); 25 μM roscovitine (Ros), except in the right hand lane (Ros +Noc) of (**D**) where roscovitine was present 1 h prior to the start and during 16 h nocodazole treatment. Proteins in the cell lysates were separated by SDS gel electrophoresis, transferred to nitrocellulose membranes, and probed with antibodies to the indicated proteins.

roscovitine,[24] our data implicate Cdk1-cyclin B because this Cdk activity increases during G_2 to a maximum at the G_2/M phase of the cell cycle and then rapidly declines. From examination of the total R2 from G_1/S to G_2/M (**Fig. 4D**) we observe a slower migration of R2 during this period, consistent with phosphorylation. R2Ser159, R2Thr173 are the phosphorylations we detect clearly at G_2/M, although additional phosphorylations cannot be excluded.

Importantly, phosphorylation of R2 from G_1/S to G_2/M is associated with an 5–10-fold decrease in endogenous Ppp4c-R2-R3A phosphatase activity during this period compared with G_1 phase and does not alter the enhanced location of Ppp4c at the centrosome during mitosis. The activity change was confirmed by Cdk1-cyclin B phosphorylation of purified Ppp4c-R2-R3A following expression of the complex in insect cells. To our knowledge this is the first report of heterologous expression of active Ppp4c or its complexes and the in vitro and in vivo regulation of Ppp4c–R2–R3A activity. Phosphorylation by Cdk1-cyclin B is consistent with earlier observations demonstrating the enrichment of Cdk1[25] and Ppp4c, R2 and R3A[9,13,17] at centrosomes during mitosis in higher eukaryotes. The essential nature of Ppp4c during nuclear divisions in *Drosophila* embryos suggests that the Ppp4c-R2-R3A will be required at this stage of the cell cycle.[10]

Current knowledge points to the nucleation of microtubules being regulated through γ-tubulin in complex with TUBGCP2 and TUBGCP3 in the γTuSC, all of which are essential for viability.[3,4,6,26] In this article we show by immunoadsorption followed by mass spectrometry and immunoblotting that endogenous Ppp4c binds to endogenous γ-tubulin and TUBGCP2. Interaction with TUBGCP3 is likely to be indirect, through γ-tubulin and/or TUBGCP2 (**Fig. 6A**). γ-tubulin can be phosphorylated by Cdk1-cyclin B on Ser80 and Thr196 and dephosphorylated by Ppp4c-R2-R3A in vitro, supporting a direct interaction between γ-tubulin and the phosphatase (**Fig. 6D and E**). Inhibition of the Ppp4c-R2-R3A activity from G_1/S to G_2/M (**Fig. 5C**) may allow initial low-level phosphorylation of γ-tubulin by Cdk1-cyclin B to nucleate the growth of short microtubules. Increase of Cdk1-cyclin B activity at G_2/M would maximally inhibit Ppp4c-R2-R3A and increase γ-tubulin phosphorylation, enhancing nucleation of microtubules and/or centrosomal attachment of microtubules necessary for forming the mitotic spindle. On exit from M-phase, decrease of the Cdk1-cyclin B activity would lead to the activation of Ppp4c-R2-R3A, enabling it to rapidly dephosphorylate γ-tubulin and maintain the dephosphorylation through G_1. This sequence of events suggests that Ppp4c-R2-R3A may play a crucial role in microtubule nucleation in all cells. An alternative explanation is that Ppp4 may regulate microtubule nucleation/attachment to the centrosomes in response to stress situations, such as mitotic spindle disruption or DNA damage. In HeLa cells treated with nocodazole, the mitotic spindle function is disrupted, but Cdk1-cyclin B remains active.[27] Consequently, Ppp4c-R2-R3A would
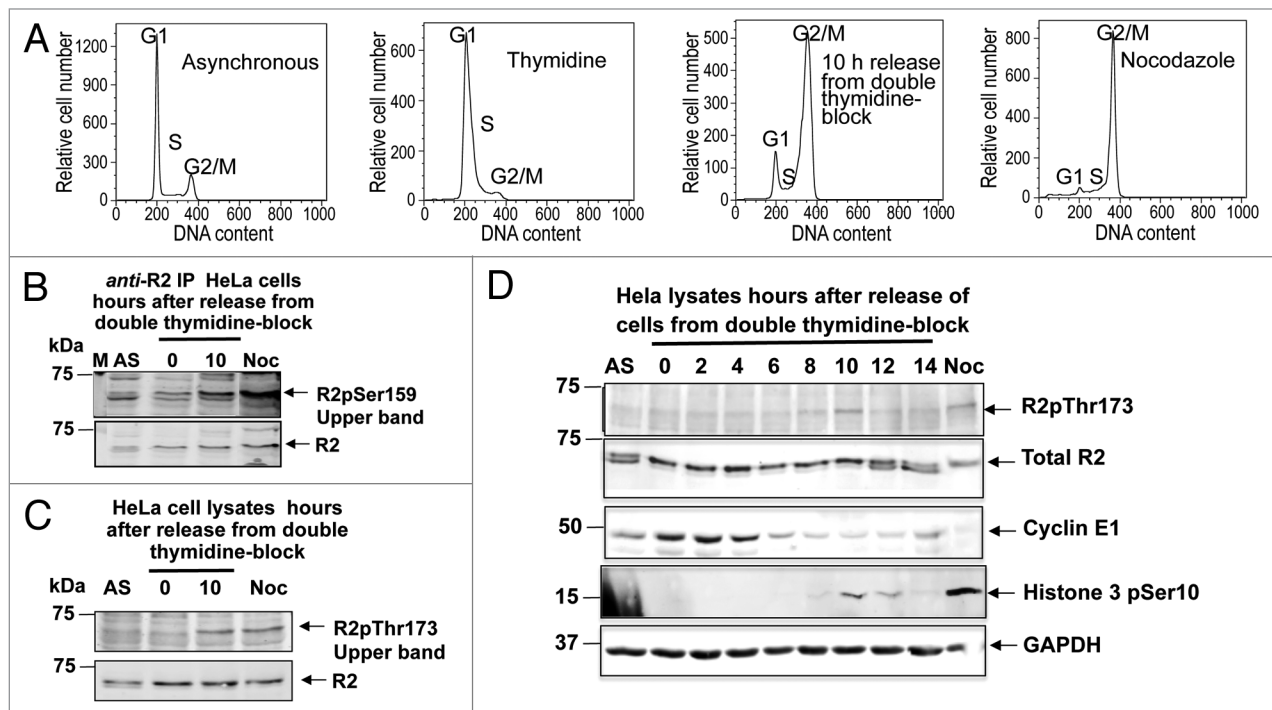

Figure 4. Phosphorylations of endogenous R2 and R3A during progression through the HeLa cell cycle. (**A**) Analysis of HeLa cells by flow cytometry shows the distribution of cells in asynchronous cultures, the same cultures immediately following the double thymidine block, 10 h after release from the double thymidine block and cell cultures blocked at G_2/M with nocodazole. (**B**) Immunoblots showing endogenous R2pSer159 in R2 immunopellets. M indicates the marker proteins, with their size in kDa. (**C**) R2pThr173 in lysates from asynchronous cultures (AS), immediately following the double thymidine block (0), 10 h after release from the double thymidine block (10) and in cells treated with nocodazole (Noc). (**D**) Immunoblot analysis of the endogenous R2, R2pThr173 and endogenous R3A during the cell cycle after a double thymidine block. Cyclin E1 detection indicates that the cells were blocked at G_1/S by thymidine and histone H3 Ser10 phosphorylation that cells were at G_2/M. GAPDH was used as a control for sample loading.

be inhibited by Cdk1-cyclin B phosphorylation. Sustained activation of Cdk1-cyclin B and inhibition of Ppp4c-R2-R3A may result in prolonged phosphorylation of γ-tubulin Ser80 and/or Thr196. Subsequent ubiquitylation of γ-tubulin may prevent the nucleation of new microtubules[28] (**Fig. 7B**). Brsk1 has been reported to phosphorylate γ-tubulin on Ser131 in response to DNA damage and inhibit Cdk1-cyclin B via phosphorylation of Cdc25 and Wee1.[21,29] In this case, Ppp4c-R2-R3A will remain active and keep γ-tubulin dephosphorylated and unable to initiate microtubule growth.

In support of Ppp4c-R2-R3A regulation in a stress situations, there have been no reports of the ortholog of Ppp4c (Pph3) in *S. cervisiae* at spindle pole bodies during mitosis, and deletion of Pph3 does not cause lethality,[30] in contrast to Ppp4c depletion in higher organisms. Neither R2Ser159, R2Thr173 nor R3ASer741 are conserved to yeast (**Fig. 7A**), which may explain why the Ppp4c-R2-R3 othologous complex is not essential for passage through G₂-M in yeast as it would be if Ppp4c-R2-R3A regulated a step in the normal cell cycle. In addition, 3 functionally important phosphorylated sites on γ-tubulin detected in yeast[31]
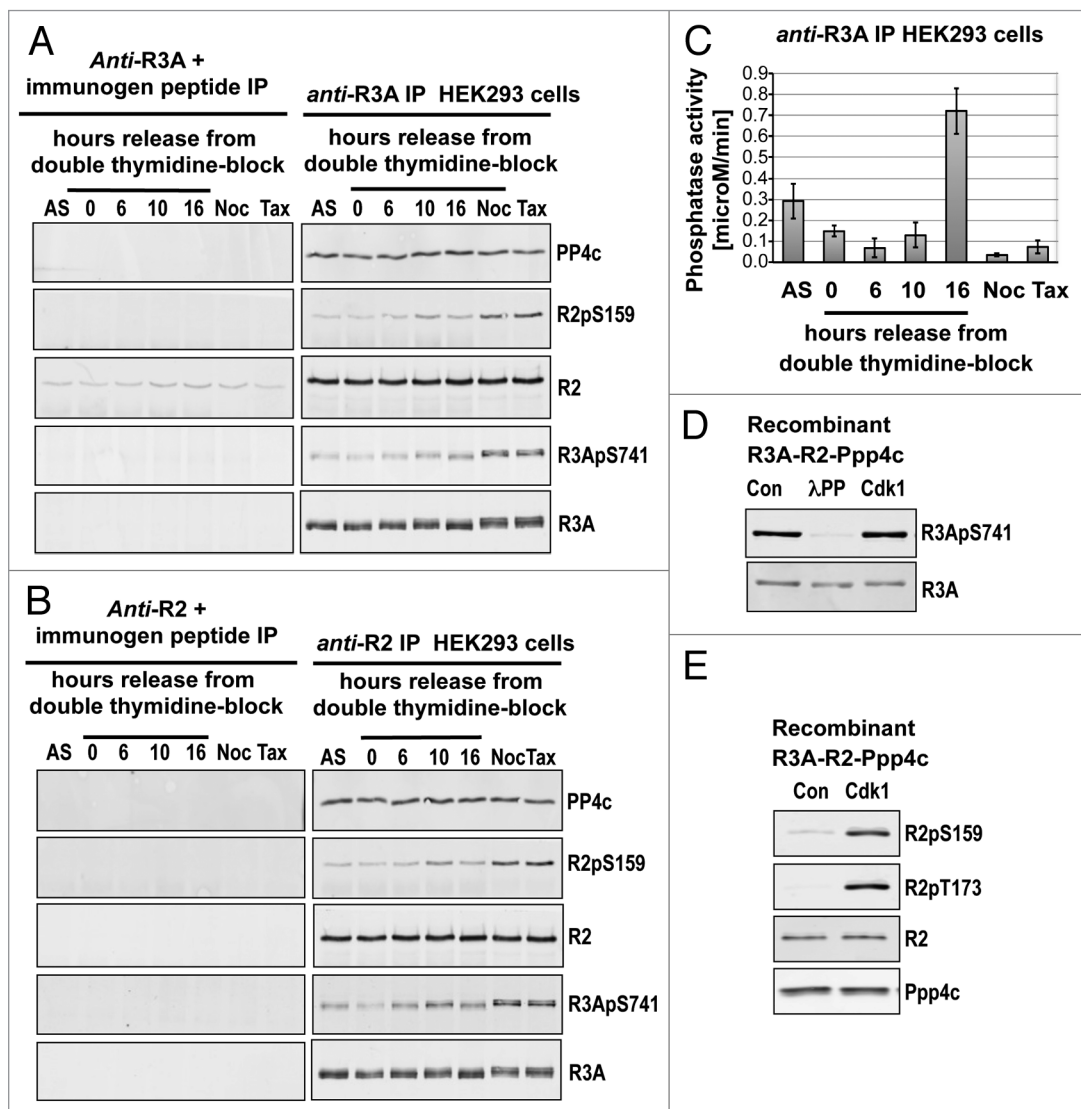

Figure 5. Phosphorylation of Ppp4 regulatory subunits and assay of endogenous Ppp4 activity during the HEK293 cell cycle. (**A**) Immunoblots showing endogenous R2pSer159 and R3pSer741 in R3A immunopellets from asynchronous cultures (AS), in cells following release from a double thymidine block and in cells treated with nocodazole (Noc) or paclitaxel (Tax). Control samples were prepared similarly except that the anti-R3A antibody was incubated with the peptide immunogen for 30 min prior to use. (**B**) Immunoblots showing endogenous R2pSer159 and R3pSer741 in R2 immunopellets from asynchronous cultures, in cells following release from a double thymidine block and in cells treated with nocodazole or paclitaxel. Control samples were prepared similarly except that the anti-R2 antibody was incubated with the peptide immunogen for 30 min prior to use. (**C**) Protein phosphatase activity was assayed in anti-R3A immunopellets from lysates of the HEK293 cells at 0, 6, 10, and 16 h after release from a double thymidine block. The phosphatase activity in the immunopellets, determined using the phosphopeptide RRApTVA as substrate. The graph shows the mean values and error bars indicate ± SD of 4 assays for each time point. (**D**) Affinity purified recombinant GST-R3A-His₆R2-Ppp4c was treated with λ phosphatase (1 μg/ml) and subsequently with Cdk1-cyclin B (1 μg/ml) at 30 °C for 30 min. and analyzed by SDS-PAGE and immunoblotting. (**E**) Recombinant GST-R3A-His₆R2-Ppp4c treated with Cdk1-cyclin B shows the phosphorylation of R2 Ser159 and R2Thr173.

were not found on human γ-tubulin treated with spindle toxins. In man, mice, and *Drosophila*, R2Ser159 is conserved, and the surrounding sequences are highly similar, while R2Thr173 and 5 amino acids on either side are identical in man and mouse. R2Thr173 is not conserved in *Drosophila*, indicating that its phosphorylation is not necessary for inhibition of Ppp4c–R2–R3A complex at G_2/M in this organism (**Fig. 7A**). R3ASer741 and the surrounding sequence are identical in man and mouse. Unambiguous alignment of the *Drosophila* R3A sequence with the mammalian sequences in this region is difficult, but putative Cdk1 sites are present in *Drosophila* R3 at Ser703, 709, and 814. A model presenting the mode of regulation of Ppp4c-R2-R3A during the cell cycle in higher eukaryotes and its putative regulation of γ-tubulin is shown in **Figure 7B**. The model suggests that an inhibitor of Ppp4c-R2-R3A would lead to sustained

phosphorylation and ubiquitylation of γ-tubulin with a block in microtubule nucleation. An inhibitor of the Ppp4 complex may therefore be beneficial in combination with paclitaxel for the treatment of certain cancers.

Materials and Methods

Cell culture and synchronization

Human embryonic kidney (HEK)293 and HeLa cervical carcinoma cell lines (supplied by the MRC-PPU tissue culture service managed by Kirsten Airey) were maintained at 37 °C in a humidified atmosphere with 5% CO_2, 95% air in Dulbecco's modified Eagle's medium (DMEM, Life Technologies, Inc., Cat. No. 11960–044) supplemented with 10% (v/v) fetal bovine serum (Sigma-Aldrich, Cat. No. F7524), 2 mM L-glutamine
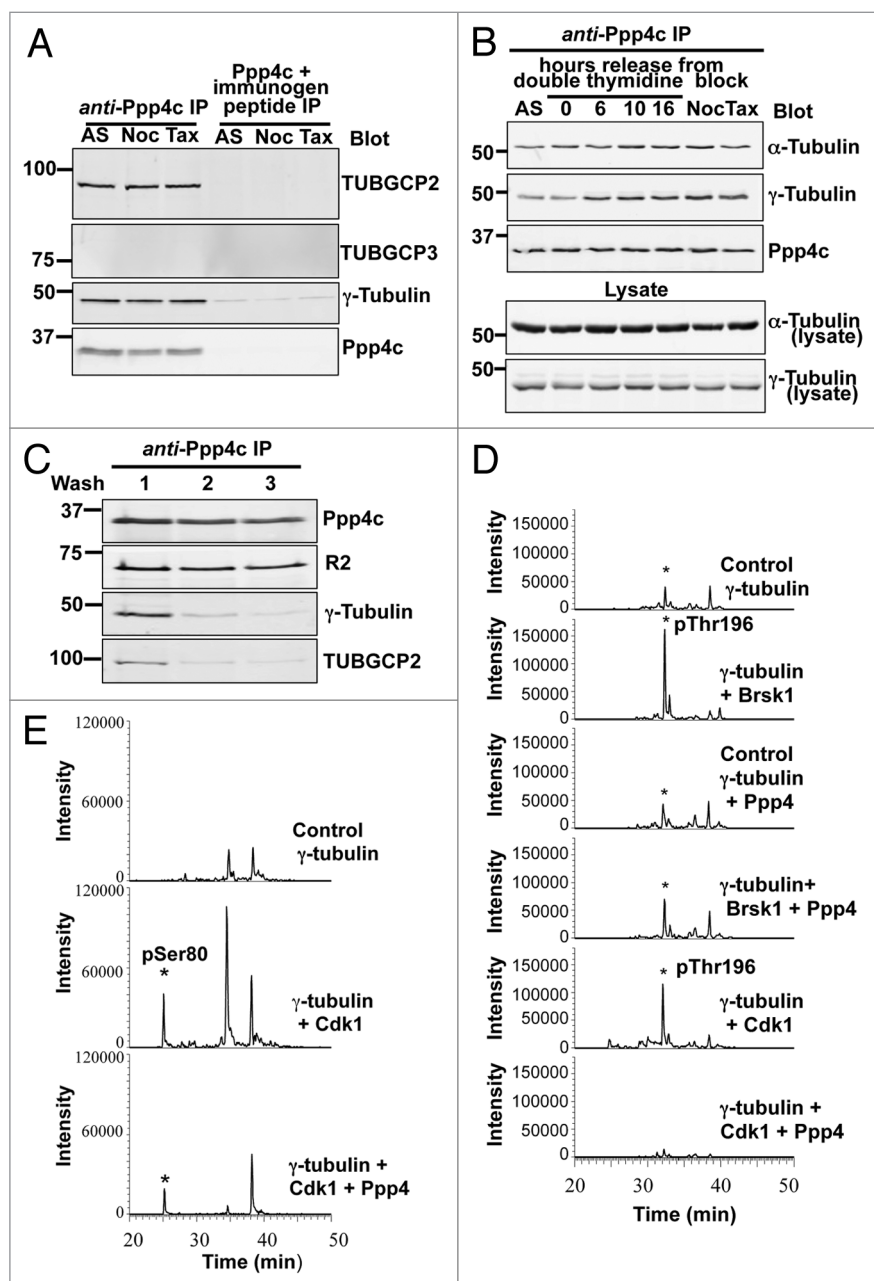

Figure 6. Identification of Ppp4c interacting proteins. (**A**) Immunoblots showing endogenous γ-tubulin and TUBGCP2 but not TUBGCP3 in immunopellets of endogenous Ppp4c complexes from lysates of asynchronous HEK293 cells (AS) or cells treated with nocodazole or paclitaxel. The control samples were prepared similarly except that the anti-Ppp4c antibody was incubated with the peptide immunogen for 30 min prior to use. (**B**) Endogenous Ppp4c complexes were immunoadsorbed using anti-Ppp4c antibody-Sepharose beads from HEK293 lysates (containing 100 nM microcystin) after release from a double thymidine cell cycle block. Proteins in the washed immunopellets were examined by SDS-PAGE. (**C**) Immunoblots showing endogenous γ-tubulin and TUBGCP2 in immunopellets of endogenous Ppp4c complexes from lysates of asynchronous HEK293 cells after 3 washes in lysis buffer [wash 1], 3 washes in lysis buffer, followed by one wash in no-salt buffer (50 mM TRIS-HCl pH 7.5, 0.1 mM DTT, 0.1 mM EGTA) and one wash in high-salt buffer (50 mM TRIS-HCl pH 7.5, 0.1 mM DTT, 500 mM NaCl) [wash 2] and 3 washes in lysis buffer, followed by 2 washes in no-salt buffer and 2 washes in high-salt buffer [wash 3]. (**D and E**) γ-tubulin was phosphorylated in vitro by Cdk1-cyclin B or Brsk1 and then dephosphorylated by Ppp4c-R2-R3A. The γ-tubulin samples were examined by SDS-PAGE and the γ-tubulin bands cut out of the gel, digested with trypsin and the peptides analyzed by mass spectrometry on an LTQ-Orbitrap Classic. (**D**) Extracted ion chromatograms (XICs) for an m/z of 699.3290 show the elution profile of a peptide identified by MSMS analysis as the phosphorylated peptide 195 L(pT)QNADCVVVLDNTALNR-212, eluting at 32.17 min (indicated by an asterisk*). The relative amounts under the different conditions were determined from the area under the relevant peak. Controls: γ-tubulin, γ-tubulin + Ppp4 complex. (**E**) XICs for an m/z of 711.3621 show the elution profile of a second phosphorylated peptide, 73-VIHSILN(pS)PYAK-84, again identified by MSMS, eluting at 25.15 min (indicated by an asterisk*). The relative amounts under the different conditions were determined from the area under the relevant peak. The peak eluting at 34.5 min could not be identified.

(Lonza, Cat. No. BE17–605E) and antibiotic-antimycotic (50 units/ml penicillin G, 0.25 µg/ml amphotericin B, 50 µg/ml streptomycin, Life Technologies, Inc., Cat. No. 15240). Cells were transfected where indicated using calcium–phosphate methodology. Where stated, cells were treated with 300 nM nocodazole (Sigma-Aldrich, Cat. No. M1404), 33 nM paclitaxel (Cell Signaling Technology, Cat. No. 9808), 25 µM roscovitine (Cell Signaling Technology, Cat. No. 9885) or 2 mM thymidine (Sigma-Aldrich, Cat. No. T1895) for 16 h. Recovery from nocodazole arrest was performed by washing in Dulbecco's
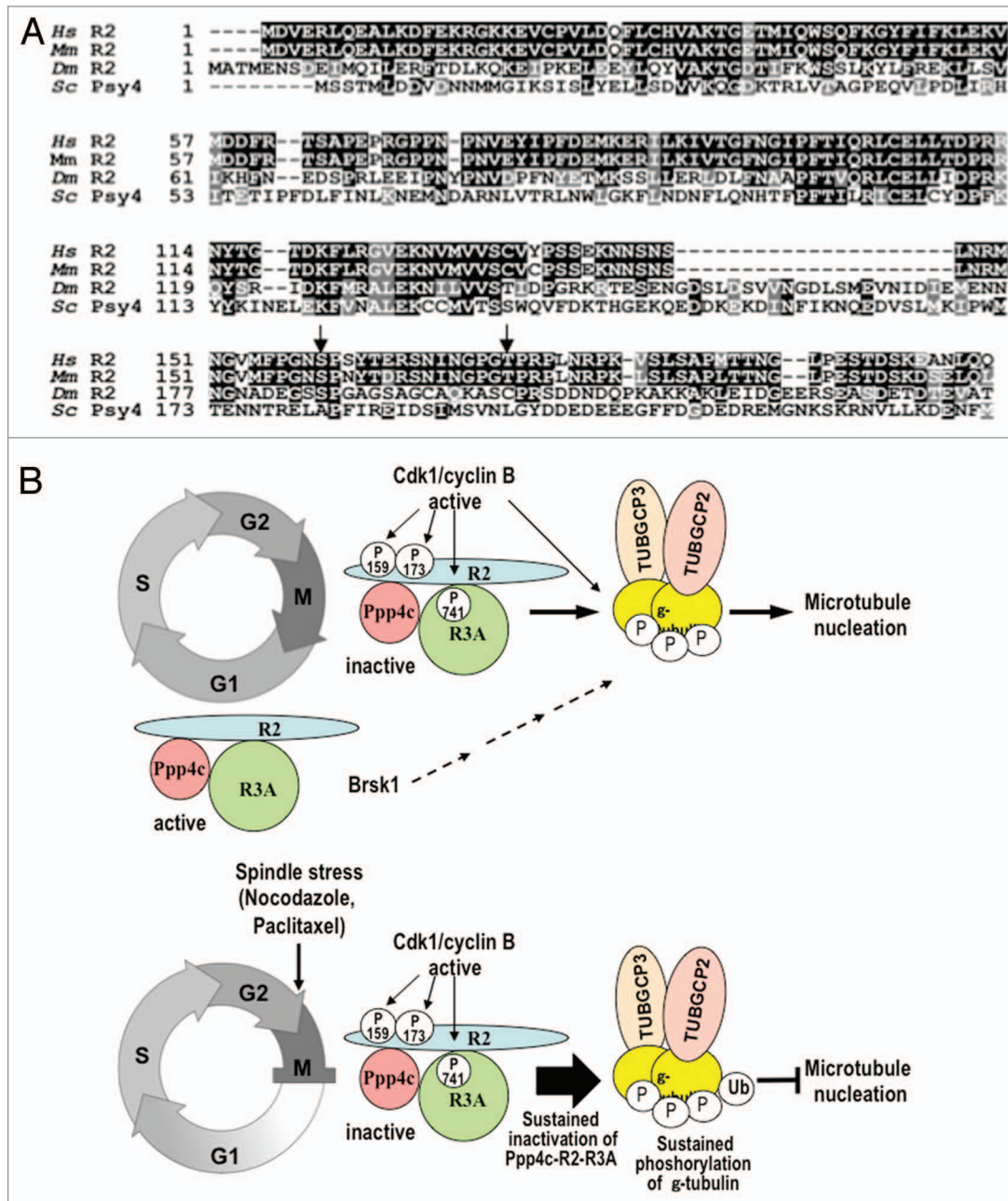

Figure 7. Regulation of the Ppp4c-R2-R3 complex by phosphorylation. (**A**) Comparison of the N-terminal half of human (*Hs*), *Mus musculus* (*Mm*), *Drosophila melanogaster* (*Dm*), and *Saccharomyces cerevisiae* (*Sc*) R2 sequences showing Ser159 and Thr173 phosphorylation sites (indicated by arrows) in human and murine R2 and the orthologous Ser phosphorylation in *Drosophila*. (**B**) Model showing the Cdk1-cyclin B phosphorylations of R2Ser159, R2Thr173 and R3ASer741, which decrease Ppp4c-R2-R3A activity between G_1/S and M-phase of the cell cycle (upper part of the figure). Ppp4c-R2-R3A interacts with γ-tubulin and TUBGCP2 (two components of γ-TuSC) keeping the protein(s) dephosphorylated in G_1, but allowing them to be phosphorylated between G_1/S and M-phase and nucleate microtubule growth, (γ-tubulin may be phosphorylated on Ser80 and Thr196). When Cdk1-cyclin B activity decreases at the end of M phase, Ppp4c-R2-R3A is dephosphorylated and activated and γ-TuSC will be dephosphorylated, inhibiting microtubule nucleation. In response to the spindle toxins, nocodazole and paclitaxel, the cell cycle is blocked at M-phase with Cdk1-cyclin B active, enabling the kinase to phosphorylate R2Ser159, R2Thr173, and R3ASer741 and inactivate Ppp4c-R2-R3A. γ-TuSC will undergo prolonged phosphorylation and may be ubiquitylated[36] because of the cell cycle block. The cell cycle then cannot proceed unless the spindle toxin is removed. Brsk1/SADB may indirectly phosphorylate γ-tubulin on Ser131.[21,37]

phosphate-buffered saline (Life Technologies, Inc. Cat. No. 14190) and incubating for 10 min at 37 °C in complete DMEM. HEK293 cell homogenates were prepared in 50 mM Tris-HCl, pH 7.5, 5% glycerol, 4 mM EDTA, 1 mM EGTA, 1 mM dithiothreitol, "Complete" protease inhibitor cocktail and 0.1 μM microcystin (Enzo Life Sciences, Cat. No. ALX-350–012) and centrifuged at 16 000 x g for 10 min. The supernatant lysate was used immediately or snap frozen and stored at -80°C.

Synchronization of cells was achieved by using a double thymidine block and release method.[32] Briefly cells were seeded at 3 x 10^6 per 15 cm diameter plate and cultured at 37 °C for 24 h. The cells were either harvested or treated with 2 mM thymidine for 16 h (thymidine I block), then washed once with PBS (to release the cells from the block) and cultured in fresh complete medium for 9 h, treated with 2 mM thymidine for 16 h (thymidine II block), then washed once in PBS and cultured in fresh complete media for the indicated times.

Mass spectrometry techniques

cDNA encoding the human R2 regulatory subunit of Ppp4 (Q9NY27, 417 amino acids) with a FLAG tag at the N-terminus was subcloned into pCMV5 for transfection into mammalian cells. FLAG-tagged R2 expressed in HEK293 cells, untreated or treated with nocodazole, was immunoadsorbed from the cell lysates using anti-FLAG M2 affinity resin (Sigma-Aldrich, Cat. No. A2220) and subjected to SDS-PAGE on 4–12% Bis-Tris gels. Following staining with colloidal Coomassie Blue, the FLAG-R2 protein was excised, alkylated, digested with trypsin (Promega Corp, Cat. No.V5280),[33] and the R2 peptides (**Fig. 1**) were analyzed for phosphorylation sites by liquid chromatography-mass spectrometry (LC-MS) with a precursor ion scan of m/z –79 on a 4000 Q TRAP instrument [Applied Biosystems].[34] Spectra were viewed using Analyst 1.4 software and the identity of each phosphorylation site was determined by a combination of Mascot searching (www.matrixscience.com) and manual interpretation of the spectra.

His$_6$-tagged γ-tubulin expressed in *E. coli* (TUBG1, Novus Biologicals, Cat. No. NBP1-72534) was bound to Ni-agarose (GE Healthcare Cat. No. 17-5318-03) in 50 mM TRIS-HCl pH 7.5, 150 mM NaCl, 0.1 mM EGTA, 1 mM DTT, 5% glycerol, "Complete" protease inhibitor Roche, Cat. No. 11836145001). Ten μg γ-tubulin bound to Ni-agarose was incubated with or without constitutively active 3 μg His$_6$-BRSK1 (aa 2–778, expressed in Sf21 cells in the Division of Signal Transduction Therapy [managed by Dr Hilary McLauchlan and Dr James Hastie]) or activated 2 μg Cdk1-Cyclin B (Merck-Millipore, Cat. No. 14-450) in a 50 μl reaction supplemented with 0.1 mM ATP at 30 °C for 30 min. Subsequently reactions were diluted 20-fold in 50 mM 3-(N-morpholino)propanesulphonic acid (MOPS) pH 7.0, 1 mM DTT, 5% glycerol, 0.01% Brij. The Ni-agarose was pelleted, and supernatant completely removed. Proteins bound to Ni-agarose were incubated with or without 20 μg/ml GST-R3A-His$_6$R2-Ppp4c complex (see below) in a 180 μl reaction in 50 mM MOPS pH 7.0, 1 mM DTT, 5% glycerol, 0.01% Brij at 30 °C for 15 min. Subsequently the Ni-agarose was pelleted and samples prepared for SDS-PAGE. Following electrophoresis, the gel was stained with colloidal coomassie blue; γ-tubulin

was excised, alkylated, and digested with trypsin. Peptides from γ-tubulin (**Fig. 6C and D**) were examined by mass spectrometric analysis performed by LC-MS-MS using a linear ion trap-orbitrap hybrid mass spectrometer (LTQ-Orbitrap Classic, Thermo Fisher Scientific) equipped with a nanoelectrospray ion source (Thermo) and coupled to a Proxeon EASY-nLC system. Data were analyzed by searching the SwissProt/Human database using Mascot. The relative amount of each phosphorylated peptide in γ-tubulin was determined from the area under the relevant peak and assessed by comparison with the same γ-tubulin phosphopeptide derived from different treatments performed and analyzed at the same time. Proteins in anti-Ppp4c immunopellets (**Fig. 6A**) were also analyzed on an LTQ-Orbitrap Classic.

Immunological techniques

Protein in cell lysates were separated by sodium dodecylsulphate PAGE (SDS-PAGE) on Tris-HCl pH 8.6 gels in Tris-glycine running buffer pH 8.3 and transferred to nitrocellulose membranes (Amersham Biosciences). The membranes were probed with primary antibodies at concentrations of approximately 1 μg/ml or at dilutions recommended by the suppliers, and phospho-specific antibodies were used in the presence of a 10-fold micromolar excess of the appropriate non-phospho peptide. The bound primary antibodies were detected using fluorescently labeled secondary antibodies in conjunction with a Li-Cor Odyssey infrared detection system (Li-Cor). Endogenous Ppp4c complexes were immunoadsorbed from cell lysates for 2 h at 4 °C with gentle mixing, using anti-Ppp4c, anti-R3A or anti-R2 antibodies covalently bound to Protein G Sepharose fast flow (GE healthcare, Cat. No. 17-0618-06). The beads were pelleted by centrifugation, washed 3 times with lysis buffer and heated at 70 °C in 50 μl NuPage lithium dodecyl sulfate sample buffer, Cat. No. NP0007), and the released proteins were examined by SDS-PAGE. Antibodies to R2(310–323)[17] R3A(819–833) and Ppp4c(287–305)[13] raised in sheep have been previously described. Antibodies to R2 149-MFPGN(pS)PSYTER-166, R2 165-INGPG(pT) PRPLNR-182, R2 400-MENDDEATEVTDEPMEQD-417, R3A 736-LSGRQS(p)PSFK-745, γ-tubulin 126-ADGSD(pS) LEGF-135 were raised in sheep and affinity purified against their respective peptides by the Division of Signal Transduction Therapy (DSTT), University of Dundee, managed by Dr Hilary McLauchlan and Dr James Hastie. Commercial primary antibodies used were anti-GAPDH (Abcam, Cat. No. ab8245), anti-TUBGCP2 (Abcam Cat. No. ab96342), and anti-TUBGCP3 (Abcam, Cat. No. ab130350), anti-FLAG M2 mouse monoclonal (Sigma-Aldrich, Cat. No. F3165), and anti-γ-tubulin mouse monoclonal (Sigma-Aldrich, Cat. No. T6557), anti-Histone H3phospho-Ser10 mouse monoclonal antibody (Cell Signaling Technology, Cat. No.3377). Peptides were synthesized by Dr Graham Bloomberg (University of Bristol).

Microscopy and image analysis

HeLa cells were seeded onto 13 mm polylysine (Sigma-Aldrich, Cat. No. P4832) coated coverslips at 60% confluence and cultured for 1 d at 37 °C and a further 18–19 h either untreated or treated with 0.3 μM nocodazole, 33 nM paclitaxel, or 25 μM roscovitine before being fixed in 4% *p*-formaldehyde (Affymetrix, Cat. No. 19943). They were then processed as

described previously.[13] DNA was stained with 4'6-diamidino-2-phenylindole (DAPI). Antibodies to human Ppp4c(287–305) raised in hens[9] and anti-R3A(819–833) antibodies raised in sheep were affinity purified from blood plasma and used to identify Ppp4c and R3A subcellular localizations. Anti-pericentrin antibodies were purchased from AbCam (Cat. No. ab4448). The primary antibodies were detected with Alexa-Fluor secondary antibodies (Life Sciences Technology) and the cells were imaged on a Zeiss LSM 700 confocal microscope.

Expression and assay of Ppp4

Constructs encoding Ppp4c, R3A with an N-terminal glutathione S-transferase (GST) epitope tag, and R2 with 6xHis at the N-terminus were cloned into the baculovirus vectors pFBDM and pFBHTb, respectively, and used to generate recombinant baculoviruses using the Bac-to-Bac system (Life Sciences Technology) following the manufacturer's protocol. Forty-eight h after infection of *Spodoptera frugiperda* 21 cells with both baculoviruses, GST-R3A-His$_6$R2-Ppp4c complex was purified from insect cells by affinity chromatography on glutathione-Sepharose 4B (GE-Healthcare, cat number 29-0081-56) by Samantha Raggett (DSTT). The protein phosphatase activity of the GST-R3A-His$_6$R2-Ppp4c complex was assayed in 50 mM Tris-HCl pH 7.5, 0.1 mM EGTA, 1 mM dithiothreitol, 0.01% (w/v) Brij-35 with 1 mM synthetic phospho-peptide RRAT(p)VA as substrate, unless otherwise specified, at 30 °C for 10 min with the release of phosphate being measured by Biomol Green (Enzo Life Sciences, Cat. No. BML-AK111). Endogenous activity of Ppp4 complexes was assayed following immunoadsorption with anti-Ppp4c(287–305) antibody from HEK293 cell lysates prepared with 100 nM okadaic acid (Merck-Millipore, Cat. No. 459618) in the lysis buffer in place of microcystin.[35] The immunopellets were rapidly washed in lysis buffer without any phosphatase inhibitors unless otherwise stated and the Ppp4 activities were assayed as described above.

References

1. Stanton RA, Gernert KM, Nettles JH, Aneja R. Drugs that target dynamic microtubules: a new molecular perspective. Med Res Rev 2011; 31:443-81; PMID:21381049; http://dx.doi.org/10.1002/med.20242

2. Oakley BR, Oakley CE, Yoon Y, Jung MK. γ-tubulin is a component of the spindle pole body that is essential for microtubule function in Aspergillus nidulans. Cell 1990; 61:1289-301; PMID:2194669; http://dx.doi.org/10.1016/0092-8674(90)90693-9

3. Kollman JM, Merdes A, Mourey L, Agard DA. Microtubule nucleation by γ-tubulin complexes. Nat Rev Mol Cell Biol 2011; 12:709-21; PMID:21993292; http://dx.doi.org/10.1038/nrm3209

4. Teixidó-Travesa N, Roig J, Lüders J. The where, when and how of microtubule nucleation - one ring to rule them all. J Cell Sci 2012; 125:4445-56; PMID:23132930; http://dx.doi.org/10.1242/jcs.106971

5. Murphy SM, Urbani L, Stearns T. The mammalian gamma-tubulin complex contains homologues of the yeast spindle pole body components spc97p and spc98p. J Cell Biol 1998; 141:663-74; PMID:9566967; http://dx.doi.org/10.1083/jcb.141.3.663

6. Meunier S, Vernos I. Microtubule assembly during mitosis - from distinct origins to distinct functions? J Cell Sci 2012; 125:2805-14; PMID:22736044; http://dx.doi.org/10.1242/jcs.092429

7. Kollman JM, Polka JK, Zelter A, Davis TN, Agard DA. Microtubule nucleating gamma-TuSC assembles structures with 13-fold microtubule-like symmetry. Nature 2010; 466:879-82; PMID:20631709; http://dx.doi.org/10.1038/nature09207

8. Erlemann S, Neuner A, Gombos L, Gibeaux R, Antony C, Schiebel E. An extended γ-tubulin ring functions as a stable platform in microtubule nucleation. J Cell Biol 2012; 197:59-74; PMID:22472440; http://dx.doi.org/10.1083/jcb.201111123

9. Brewis ND, Street AJ, Prescott AR, Cohen PTW. PPX, a novel protein serine/threonine phosphatase localized to centrosomes. [and p2231]. EMBO J 1993; 12:987-96; PMID:8384557

10. Helps NR, Brewis ND, Lineruth K, Davis T, Kaiser K, Cohen PTW. Protein phosphatase 4 is an essential enzyme required for organisation of microtubules at centrosomes in Drosophila embryos. J Cell Sci 1998; 111:1331-40; PMID:9570751

11. Sumiyoshi E, Sugimoto A, Yamamoto M. Protein phosphatase 4 is required for centrosome maturation in mitosis and sperm meiosis in C. elegans. J Cell Sci 2002; 115:1403-10; PMID:11896188

12. Shui JW, Hu MC, Tan TH. Conditional knockout mice reveal an essential role of protein phosphatase 4 in thymocyte development and pre-T-cell receptor signaling. Mol Cell Biol 2007; 27:79-91; PMID:17060460; http://dx.doi.org/10.1128/MCB.00799-06

13. Martin-Granados C, Philp A, Oxenham SK, Prescott AR, Cohen PTW. Depletion of protein phosphatase 4 in human cells reveals essential roles in centrosome maturation, cell migration and the regulation of Rho GTPases. Int J Biochem Cell Biol 2008; 40:2315-32; PMID:18487071; http://dx.doi.org/10.1016/j.biocel.2008.03.021

14. Cohen PTW, Philp A, Vázquez-Martin C. Protein phosphatase 4--from obscurity to vital functions. FEBS Lett 2005; 579:3278-86; PMID:15913612; http://dx.doi.org/10.1016/j.febslet.2005.04.070

15. Gingras AC, Caballero M, Zarske M, Sanchez A, Hazbun TR, Fields S, Sonenberg N, Hafen E, Raught B, Aebersold R. A novel, evolutionarily conserved protein phosphatase complex involved in cisplatin sensitivity. Mol Cell Proteomics 2005; 4:1725-40; PMID:16085932; http://dx.doi.org/10.1074/mcp.M500231-MCP200

16. Vázquez-Martin C, Rouse J, Cohen PTW. Characterization of the role of a trimeric protein phosphatase complex in recovery from cisplatin-induced versus noncrosslinking DNA damage. FEBS J 2008; 275:4211-21; PMID:18647348; http://dx.doi.org/10.1111/j.1742-4658.2008.06568.x

17. Hastie CJ, Carnegie GK, Morrice N, Cohen PTW. A novel 50 kDa protein forms complexes with protein phosphatase 4 and is located at centrosomal microtubule organizing centres. Biochem J 2000; 347:845-55; PMID:10769191; http://dx.doi.org/10.1042/0264-6021:3470845

18. Carnegie GK, Sleeman JE, Morrice N, Hastie CJ, Peggie MW, Philp A, Lamond AI, Cohen PTW. Protein phosphatase 4 interacts with the Survival of Motor Neurons complex and enhances the temporal localisation of snRNPs. J Cell Sci 2003; 116:1905-13; PMID:12668731; http://dx.doi.org/10.1242/jcs.00409

19. Nogales E, Wolf SG, Downing KH. Structure of the alpha beta tubulin dimer by electron crystallography. Nature 1998; 391:199-203; PMID:9428769; http://dx.doi.org/10.1038/34465

20. Amos LA, Löwe J. How Taxol stabilises microtubule structure. Chem Biol 1999; 6:R65-9; PMID:10074470; http://dx.doi.org/10.1016/S1074-5521(99)89002-4

21. Alvarado-Kristensson M, Rodríguez MJ, Silió V, Valpuesta JM, Carrera AC. SADB phosphorylation of gamma-tubulin regulates centrosome duplication. Nat Cell Biol 2009; 11:1081-92; PMID:19648910; http://dx.doi.org/10.1038/ncb1921

22. Dephoure N, Zhou C, Villén J, Beausoleil SA, Bakalarski CE, Elledge SJ, Gygi SP. A quantitative atlas of mitotic phosphorylation. Proc Natl Acad Sci U S A 2008; 105:10762-7; PMID:18669648; http://dx.doi.org/10.1073/pnas.0805139105

23. Molina H, Horn DM, Tang N, Mathivanan S, Pandey A. Global proteomic profiling of phosphopeptides using electron transfer dissociation tandem mass spectrometry. Proc Natl Acad Sci U S A 2007; 104:2199-204; PMID:17287340; http://dx.doi.org/10.1073/pnas.0611217104

24. Wesierska-Gadek J, Borza A, Walzi E, Krystof V, Maurer M, Komina O, Wandl S. Outcome of treatment of human HeLa cervical cancer cells with roscovitine strongly depends on the dosage and cell cycle status prior to the treatment. J Cell Biochem 2009; 106:937-55; PMID:19180585; http://dx.doi.org/10.1002/jcb.22074

25. Jackman M, Lindon C, Nigg EA, Pines J. Active cyclin B1-Cdk1 first appears on centrosomes in prophase. Nat Cell Biol 2003; 5:143-8; PMID:12524548; http://dx.doi.org/10.1038/ncb918

26. Xiong Y, Oakley BR. In vivo analysis of the functions of gamma-tubulin-complex proteins. J Cell Sci 2009; 122:4218-27; PMID:19861490; http://dx.doi.org/10.1242/jcs.059196

27. Chan YW, Ma HT, Wong W, Ho CC, On KF, Poon RY. CDK1 inhibitors antagonize the immediate apoptosis triggered by spindle disruption but promote apoptosis following the subsequent rereplication and abnormal mitosis. Cell Cycle 2008; 7:1449-61; PMID:18418077; http://dx.doi.org/10.4161/cc.7.10.5880

28. Sankaran S, Crone DE, Palazzo RE, Parvin JD. BRCA1 regulates gamma-tubulin binding to centrosomes. Cancer Biol Ther 2007; 6:1853-7; PMID:18087219; http://dx.doi.org/10.4161/cbt.6.12.5164

29. Lu R, Niida H, Nakanishi M. Human SAD1 kinase is involved in UV-induced DNA damage checkpoint function. J Biol Chem 2004; 279:31164-70; PMID:15150265; http://dx.doi.org/10.1074/jbc.M404728200

30. Ronne H, Carlberg M, Hu G-Z, Nehlin JO. Protein phosphatase 2A in Saccharomyces cerevisiae: effects on cell growth and bud morphogenesis. Mol Cell Biol 1991; 11:4876-84; PMID:1656215

31. Lin TC, Gombos L, Neuner A, Sebastian D, Olsen JV, Hrle A, Benda C, Schiebel E. Phosphorylation of the yeast γ-tubulin Tub4 regulates microtubule function. PLoS One 2011; 6:e19700; PMID:21573187; http://dx.doi.org/10.1371/journal.pone.0019700

32. Cude K, Wang Y, Choi HJ, Hsuan SL, Zhang H, Wang CY, Xia Z. Regulation of the G2-M cell cycle progression by the ERK5-NFkappaB signaling pathway. J Cell Biol 2007; 177:253-64; PMID:17452529; http://dx.doi.org/10.1083/jcb.200609166

33. Shevchenko A, Tomas H, Havlis J, Olsen JV, Mann M. In-gel digestion for mass spectrometric characterization of proteins and proteomes. Nat Protoc 2006; 1:2856-60; PMID:17406544; http://dx.doi.org/10.1038/nprot.2006.468

34. Williamson BL, Marchese J, Morrice NA. Automated identification and quantification of protein phosphorylation sites by LC/MS on a hybrid triple quadrupole linear ion trap mass spectrometer. Mol Cell Proteomics 2006; 5:337-46; PMID:16260767; http://dx.doi.org/10.1074/mcp.M500210-MCP200

35. Cohen PTW, Browne GJ, Delibegovic M, Munro S. Assay of protein phosphatase 1 complexes. Methods Enzymol 2003; 366:135-44; PMID:14674246; http://dx.doi.org/10.1016/S0076-6879(03)66012-X

36. Parvin JD. The BRCA1-dependent ubiquitin ligase, gamma-tubulin, and centrosomes. Environ Mol Mutagen 2009; 50:649-53; PMID:19274767; http://dx.doi.org/10.1002/em.20475

37. Carrera AC, Alvarado-Kristensson M. SADB kinases license centrosome replication. Cell Cycle 2009; 8:4005-6; PMID:19949293; http://dx.doi.org/10.4161/cc.8.24.10178